Real space tomography of the primordial Universe with cluster polarization

L. Raul Abramo* and Henrique S. Xavier
Instituto de Física, Universidade de São Paulo
CP 66318, 05315-970, São Paulo, Brazil

We describe how a survey of the polarization of the cosmic microwave background induced by Compton scattering in galaxy clusters can be used to make a full spatial reconstruction of the primordial ($z \sim 1089$) matter distribution inside our surface of last scattering. This "polarization tomography" can yield a spatial map of the initial state of the Universe just as gravitational collapse was beginning to drive structure formation. We present a transparent method and simple formulas from which one can compute the 3D primordial map in real and in Fourier space, given a 3D map of the polarization due to galaxy clusters. The advantage of the real space reconstruction is that it is free from the statistical uncertainties which are inherent in the Fourier space reconstruction. We discuss how noise, partial sky covering and depth of the survey can affect the results.

PACS numbers: 98.65.Cw, 98.70.Vc, 98.80.-k, 98.80.Es

Introduction The latest observations of the cosmic microwave background (CMB) [1, 2] and of the galaxy distribution in the low-redshift Universe [3, 4] have shown a spectacular agreement with the standard theory of structure formation [5, 6]. In this scenario, the initial conditions were set up by inflation, which created a nearly scale-invariant spectrum of Gaussian density perturbations with tiny variance ($\sigma \sim 10^{-5}$), and all the visible structure we see today developed through gravitational instability from the inflationary seeds.

However, these two sets of observations are made at two very different moments in time, and they probe very different regions of space: while the CMB is formed essentially through the Sachs-Wolfe effect at the time of recombination ($z \sim 1089$), galaxies on the other hand are observed only in relatively recent times ($z \lesssim 5$.) Moreover, the CMB gives us a picture of the thin spherical shell known as the last scattering surface (LSS), which corresponds to the original location, at the time of recombination, of the CMB photons we observe on Earth today, while the galaxy distribution, in practice, can only be observed well inside our LSS. This fact leads to a statistical "leap of faith" in the argument for the standard scenario: we believe that the matter distribution *inside* our LSS is similar to the matter distribution *on* our LSS, and therefore a typical configuration for the matter distribution at $z \sim 1089$ would lead to a map of the large-scale structure at $z \lesssim 5$ which has similar statistical properties to the one we actually observe. This leap can be a particularly long one if the CMB anisotropies, which provide a picture of the matter distribution on our LSS, shows suspicious anomalies [7, 8, 9, 10, 11, 12, 13, 14, 15, 16, 17, 18, 19].

Kamionkowski and Loeb [20] were the first to realize that it is possible, in principle, to recover information about the primordial matter distribution inside our LSS using cluster polarization of the CMB – see also [21, 22, 23, 24, 25]. This is because the CMB photons, as they Compton-scatter on free electrons in a galaxy cluster (the Sunyaev-Zel'dovich effect – see [26, 27]), acquire a polarization which reflects the quadrupole of the temperature distribution of the incident photons [28]. Hence, observing the polarization pattern in a galaxy cluster is tantamount to observing the quadrupole of the CMB in the LSS seen by that cluster. In principle, this means that by sampling all the LSS's of clusters inside our LSS through cmb polarization, we could reconstruct the temperature distribution of photons in the whole volume inside our LSS, and thus reconstruct the matter distribution in that volume – see Fig. 1.

Notice that a similar argument could be made for the CMB polarization which is induced at the time of last scattering through the local temperature quadrupole as well as for the polarization from the epoch of reionization. However, the former is highly degenerate with the information we already have from the CMB temperature itself (see [29] for a reconstruction scheme based on the CMB temperature), and the latter is a large-scale effect which is widely spread over the line of sight (as the ionization depth in this case is only significant over horizon-scale distances), making it difficult to trace the polarized photons back to a particular spacetime event over the past light-cone. Nevertheless, if reionization is patchy and inhomogeneous, polarization combined with 21-cm observations can be used much in the same way as cluster polarization to reconstruct the primordial matter distribution [30] – and formulas very similar to the ones we show here can be used in that case as well.

In practice, the reconstruction scheme based on cluster polarization has been difficult to implement for several reasons. First and foremost, because the amplitude of the polarized signal is at most a few percent of the temperature fluctuation signal for typical cluster optical depths [28, 31, 32, 33]. Second, foregrounds such as lensing [34], extended galactic emissions [35, 36, 37], cluster peculiar velocities [38, 39] and filamentary structures [31], can be hard to extricate from the data. And third, the methods for recovering the matter distribution from polarization maps lacked transparency [21, 23, 24].

*Electronic address: abramo@fma.if.usp.br

We believe that these difficulties will be overcome. First, the latest technological advances have made it possible to start searching for the B-mode of polarization induced by gravitational waves from inflation [40, 41, 42, 43] – which will be more than enough sensitivity to detect polarization at the levels found in clusters. Optic and X-ray data, which are crucial to determine the optical depths and redshifts of the clusters, should make de-lensing significantly easier at the arcminute scales we are interested [44, 45]. Filamentary structures can be avoided by cutting out regions of the sky with very high gas columns or projected surface density of clusters. Similarly, galactic foregrounds can be either directly subtracted with multi-frequency observations, or a mask can be applied onto the maps. Cluster peculiar velocities can also be dealt with in multi-frequency surveys [22].

As for the reconstruction of the matter distribution, we will present a transparent method and simple formulas for the reconstruction of the matter distribution both in Fourier as well as in real space. We have considered the contributions from the Sachs-Wolfe and the integrated Sachs-Wolfe effects (SWe and ISWe, respectively). It is trivial to consider surveys with partial sky covering, as well as any type of redshift binning one may employ. We also study the effect of adding noise to the polarization data and its impact on the reconstructed maps.

Cluster polarization Since only the Stokes parameters Q and U are relevant in cosmology [46, 47, 48], we define the dimensionless complex polarization of a cluster at redshift z in the direction $\hat{n}$ as:

$$P(z,\hat{n}) \equiv \frac{Q(z,\hat{n}) - i\,U(z,\hat{n})}{T(z)\tau_{z,\hat{n}}} \,, \qquad (1)$$

where $T(z) = 2.726(1+z)$ K and $\tau_{z,\hat{n}}$ is the optical depth for the cluster at redshift z and position $\hat{n}$.

At linear order in the cosmological perturbations (we neglect the Riess-Sciama effect), the polarization for a given cluster depends on the gravitational potential Φ *on* the cluster's LSS through the SWe, and it depends on the fluctuations of the potential *inside* the cluster's LSS through the ISWe – see Fig. 1.

Usually one describes the gravitational potential in terms of its Fourier spectrum:

$$\Phi[\vec{r}(z,\hat{n})] = \int \frac{d^3k}{(2\pi)^{3/2}} e^{-i\vec{k}\cdot\vec{r}} \tilde{\Phi}(\vec{k}) \,. \qquad (2)$$

The Fourier transform of the gravitational potential has Gaussian random P.D.F.'s set up by inflation, with $\langle\tilde{\Phi}(\vec{k})\tilde{\Phi}^*(\vec{k}')\rangle = k^{-3}P(k)\delta(\vec{k}-\vec{k}')$, and $P(k) = Ak^{n_s-1}$ a nearly scale-invariant function.

For this problem it is very useful to describe the gravitational potential in the volume inside our LSS (which includes the LSS's of all clusters) in the following way:

$$\Phi(\vec{r}) = \sum_{\ell,m} b_{\ell m}(r)\, Y_{\ell m}(\hat{n}) \,, \qquad (3)$$

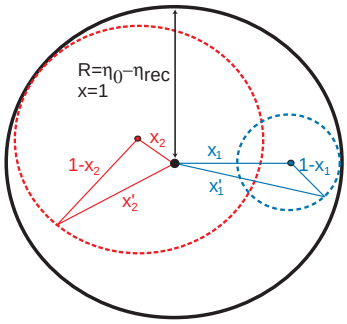

FIG. 1: Last scattering surfaces seen by an observer at the origin at $\eta = \eta_0$ (solid black circle) and by two clusters at times η_1 and η_2 (dashed grey circles – dashed red and blue circles in the online version.) The variable x is physical distance in units of the distance to our LSS, $x = (\eta - \eta_{rec})/(\eta_0 - \eta_{rec})$. The distance from the origin to the LSS of a given cluster at x spans the interval $|1-2x| \leq x' \leq 1$.

where $r = \eta_0 - \eta(z)$ and η is conformal time. The coefficients $b_{\ell m}(r)$ are well-behaved functions of the radius if $\Phi(\vec{r})$ is a smooth function. Since the radius of our LSS, at $z_{\rm rec} \simeq 1089$, is $R_{\rm LSS} = \eta_0 - \eta_{\rm rec}$, it is useful to write all physical distances in terms of this maximal radius, $x \equiv r/R_{\rm LSS}$ so x lies in the interval $0 \leq x \leq 1$.

We can write $\tilde{\Phi}(\vec{k})$ in the same way as Eq. (3), in terms of coefficients $\tilde{b}_{\ell m}(k)$. The formal relationship between $b_{\ell m}(x)$ and $\tilde{b}_{\ell m}(k)$ is a Hankel transform:

$$\tilde{b}_{\ell m}(k) = \sqrt{\frac{2}{\pi}}\,(-i)^\ell \int dx\, x^2\, j_\ell(kx)\, b_{\ell m}(x) \,. \qquad (4)$$

The inverse relation is found by exchanging $k \leftrightarrow x$ and multiplying by $(-1)^\ell$. The fact that $\Phi(\vec{r})$ is real translates into the conditions $\tilde{b}^*_{\ell m} = (-1)^{\ell+m}\tilde{b}_{\ell,-m}$ and $b^*_{\ell m} = (-1)^m b_{\ell,-m}$.

A decomposition analogous to Eq. (3) can be made for the cluster polarization as well, except that here the spin-2 character of the polarization field demands that we use the spin-weighted spherical harmonics instead [25]:

$$P = \sum_{\ell,m} p_{\ell m}(x)\, {}_2Y_{\ell m}(\hat{n}) \,. \qquad (5)$$

In terms of the coefficients $p_{\ell m}(x)$ and $\tilde{b}_{\ell m}(k)$, the cluster polarization takes on a very simple expression:

$$p_{\ell m}(x) = \int dk\, \tilde{K}_\ell(x,k)\, \tilde{b}_{\ell m}(k) \,, \qquad (6)$$

where the Fourier space Kernel $\tilde{K}_\ell(x,k)$ is given by:

$$\tilde{K}_\ell(x,k) = i^\ell\, 60\pi \sqrt{\frac{3}{2}}\, k^2\, f_\ell(kx)\, \tilde{\Delta}_2(x,k) \,, \qquad (7)$$

with [25]:

$$f_\ell(kx) = -\frac{1}{45}\sum_{\lambda=\ell-2,\ell,\ell+2}(-1)^{(\lambda-\ell)/2}(2\lambda+1) \times \begin{pmatrix} 2 & \ell & \lambda \\ 2 & -2 & 0 \end{pmatrix}\begin{pmatrix} 2 & \ell & \lambda \\ 0 & 0 & 0 \end{pmatrix} j_\lambda(kx)\ , \quad (8)$$

and

$$\tilde{\Delta}_2(x,k) = j_2[k(1-x)] - 6\int_x^1 dx'' j_2[k(x''-x)]\frac{dG(x'')}{dx''}\ . \quad (9)$$

The first and second terms in Eq. (9) stand for, respectively, the SWe and the ISWe. The growth function $G(x) = D[z(x)]/a[z(x)]$ is normalized to unity today and its derivative is non-negligible only in relatively recent times ($z \lesssim 5$) as dark energy becomes more relevant.

In fact, it turns out that the sum in Eq. (8) is a particular realization of the spherical Bessel function's recursion relations, and the result is:

$$f_\ell(kx) = \sqrt{\frac{(\ell+2)!}{6(\ell-2)!}}\,\frac{j_\ell(kx)}{30(kx)^2}\ . \quad (10)$$

This window function, which mediates the exchange of power between the "orbit" angular momenta $\ell \geq 2$ and the spin angular momentum of the polarization field, is identical to the one found in Ref. [24] for the correlation function of the polarization coefficients, and it ensures that the power is conserved, $\sum_{\ell=2}^{\infty}(2\ell+1)f_\ell^2 = 1$. It is also the same (up to a normalization factor) as the radial function $\epsilon_\ell^{(0)}$ of [48], which shows that the cluster-induced polarization is a pure E (or gradient) mode.

Polarization tomography in real space Even perfect knowledge of the polarization field on the whole volume of our LSS does not eliminate the statistical errors in the Fourier space coefficients $\tilde{b}_{\ell m}(k)$ – as Eq. (4) is cut-off at $x = 1$. These uncertainties are a 3D analog of the 2D "cosmic variance" that plagues CMB anisotropies. However, even though these statistical uncertainties can be large, especially for the longest-wavelength modes, we can still reconstruct the 3D spatial map of the primordial fluctuations inside the LSS with as much accuracy as the observations allow. This is a nontrivial statement, as the polarization we observe from a cluster carries only the information of the temperature quadrupole as seen by that cluster, projected along the line of sight. Nevertheless, it turns out that this is just enough information to allow (at least in theory) for a complete spatial reconstruction.

Plugging Eq. (4) into Eq. (6) and using a generalization of the Weber-Shafheitlin integral [49] we obtain:

$$p_{\ell m}(x) = \int_0^1 dx'\, K_\ell(x,x') b_{\ell m}(x')\ , \quad (11)$$

where the real space kernel $K_\ell(x,x')$ is given by an SWe piece and an ISWe piece. It turns out that K_ℓ is real, which is another manifestation of the fact that cluster polarization is a pure E mode.

The SWe kernel is:

$$K_\ell^{(SW)} = \frac{\pi^2}{2}\sqrt{\frac{(\ell+2)!}{2\pi(\ell-2)!}}\,\frac{x'^3}{x(1-x)^3} \times \theta(|x'+x|-|1-x|)]\,\theta(|1-x|-|x'-x|) \times \sin^2\psi\, P_\ell^{-2}(\cos\psi)\ , \quad (12)$$

where P_ℓ^n is the generalized Legendre polynomial, and $\cos\psi = [x^2+x'^2-(1-x)^2]/(2xx')$ is the cosine of the angle between x and x' in a triangle with sides x, x' and $1-x$ – see Fig. 1. The step-functions in Eq. (12), which vanish unless $|1-2x| \leq x' \leq 1$, automatically imply causality and ensure that the polarization in each point can only depend, through the SWe, on the gravitational potential on the LSS of that point.

The ISWe part is given by:

$$K_\ell^{(ISW)} = -3\pi^2\sqrt{\frac{(\ell+2)!}{2\pi(\ell-2)!}}\,\frac{x'^3}{x}\int_x^1 dx''\frac{1}{(x''-x)^3} \times \theta(|x'+x|-|x''-x|)]\,\theta(|x''-x|-|x'-x|) \times \frac{dG(x'')}{dx''}\sin^2\psi'\, P_\ell^{-2}(\cos\psi')\ , \quad (13)$$

where $\cos\psi' = [x^2+x'^2-(x''-x)^2]/(2xx')$ is the cosine of the angle between x and x' in the triangle with sides x, x' and $x''-x$. As was the case for the SWe kernel above, it is straightforward to show from the step-functions in Eq. (13) that the ISWe kernel vanishes if $x' > 1$. Detailed geometric interpretations of the real space kernels can be found in a forthcoming publication [50].

Notice that by virtue of the step-functions in the kernels above, the variables x, x' and x'' all lie in the interval $[0,1]$, so both $p_{\ell m}$ and $b_{\ell m}$ have compact support. This means that the linear problem of finding the coefficients $b_{\ell m}(x')$ given the data $p_{\ell m}(x)$ is completely well-defined in real space. This is in contrast with the problem of finding the Fourier space coefficients $\tilde{b}_{\ell m}$ given the same data: because the $p_{\ell m}$'s in Eq. (6) can only be integrated over the interval $0 \leq x \leq 1$, the inversion of Eq. (6) is singular. Evidently, this is a manifestation of the statistical uncertainties of the $\tilde{b}_{\ell m}$'s.

Eqs. (11)-(13) are the main results of this paper. Next we discuss applications of these formulas.

Map reconstruction In practice, the integrals (6) and (11) become sums over bins, so we have to solve a linear problem of the type $P_{\ell m\,(i)} = \sum_j K_{\ell\,(ij)} B_{\ell m\,(j)}$, with K_ℓ some matrix that need not be square if we want to compute less parameters $B_{\ell m\,(j)}$ than there are data points $P_{\ell m\,(i)}$. But even if the matrix K_ℓ is square, in general it is singular. This is a severe problem for the Fourier space kernel, which has many singular eigenvalues due to the statistical uncertainties in the long-wavelength modes $\lambda \gtrsim R_{\rm LSS}$ [50]. For the real space kernel we find that there are essentially no singular eigenvalues, which allows, at least in principle, for an exact inversion.

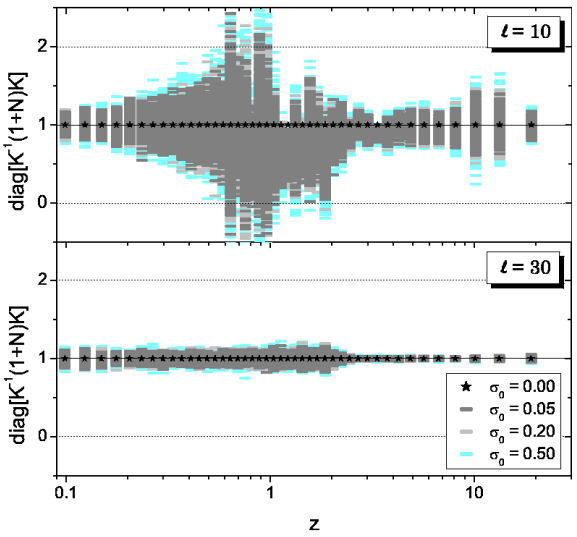

FIG. 2: Noisy estimator $K_\ell^+(\mathbb{1}+N_\ell)K_\ell$ for $\ell = 10$ (top) and $\ell = 30$ (bottom), assuming zero errors (black stars) and assuming Gaussian errors with variances $\sigma_0 = 0.05, 0.2, 0.5$ (boxes of dark, medium and light grey.) We used 500 realizations of N_ℓ for each σ_0, and we use $f_{\rm sky} = 2/3$. In this example we have assumed a hypothetical survey with 100 redshift bins up to $z = 10$, and we recover information on 50 redshift bins.

For linear problems which involve rectangular or singular square matrices, we can employ the pseudo-inverse [51]. The pseudo-inverse K^+ of a matrix K reduces to the inverse in the case of square non-singular matrices, and it gives the least-squares solution $\hat{B} = K^+ \cdot P$ to the linear problem $P = K \cdot B$. In this framework it is trivial to consider noisy data: the observations become $P_{\ell m} \to P^N_{\ell m} = (\mathbb{1}+N_\ell)\cdot P_{\ell m}$, where N_ℓ is the noise matrix which is diagonal if the errors are uncorrelated.

In the presence of noisy data the estimator $\hat{B}_{\ell m}$ becomes a noisy estimator $\hat{B}^N_{\ell m}$, which can be related to the actual parameters $B_{\ell m}$ that we want to measure by:

$$\hat{B}^N_{\ell m} = K_\ell^+(\mathbb{1}+N_\ell)K_\ell \cdot B_{\ell m} \; . \qquad (14)$$

Here N_ℓ is a Gaussian random variable with zero mean and variance given by:

$$\sigma_\ell \approx \sqrt{\frac{2}{2\ell+1}\frac{1}{f_{\rm sky}}}\left(1 - f_{\rm sky} + \sigma_0^2\right)^{1/2} \; , \qquad (15)$$

where σ_0 includes factors such as instrument noise, number of pixels and redshift, and $f_{\rm sky} \leq 1$ is the fraction of the sky mapped by that instrument. The term $f_{\rm sky}$ inside the parenthesis in Eq. (15) subtracts cosmic variance, which is not relevant for the accuracy of the actual map reconstruction.

Since for the real space kernel K^+K is nearly identical to the unit matrix (unlike the case of the Fourier space kernel), one can easily find that the covariance matrix of the estimator $\hat{B}^N_{\ell m}$ is given by:

$$Cov(\hat{B}^N_{\ell m})_{ij} \simeq \sigma_\ell^2 \delta_{ij} \sum_k B_{\ell m\, k} B^*_{\ell m\, k} \; . \qquad (16)$$

One can recognize the sum over redshift bins in the r.h.s. of Eq. (16) as the projected C_ℓ – i.e., $\int dz\, C_\ell(z)$.

If the matrix $K_\ell^+(\mathbb{1}+N_\ell)K_\ell$ is close to a unit matrix, then the noisy estimator will be a good approximation to the true parameters. We can evaluate the goodness of the noisy estimator by looking at the diagonal of that matrix.

We have done this for all the modes between $\ell = 2$ and $\ell = 50$, using errors $\sigma_0 = 0.05, 0.2, 0.5$, in a hypothetical survey up to $z = 10$ with 100 bins, and in which we reconstruct the $b_{\ell m}$'s in 50 redshift bins. In this example, for $\ell = 2$ the reconstruction fails, mainly because of poor sky coverage. However, as ℓ increases sky coverage becomes less of a problem and the reconstruction becomes progressively better. Fig. 2 shows the accuracy of the reconstruction for $\ell = 10$ and $\ell = 30$. A deeper survey does not significantly improve the reconstruction, but a survey shallower than $z \lesssim 3$ impacts negatively the reconstruction at low redshifts, as the LSS's of low-redshift clusters are entirely at high redshifts. The severest limitation to the reconstruction scheme is sky coverage.

Conclusions We have shown how to reconstruct the primordial density field inside our LSS using cluster polarization. In principle, a complete reconstruction is possible with this method. In practice, sky coverage and noise limit the accuracy of the reconstruction, especially for low ℓ's and for intermediate redshifts ($z \sim 1$). Nevertheless, a reconstruction of the primordial density field in the local Universe ($z \lesssim 0.5$) and on angular scales $2^o \lesssim \theta \lesssim 20^o$, is feasible with the next generation of polarimeters which are being used to search for the B mode from gravitational waves.

The primordial field is highly correlated with the present matter distribution. Direct comparison of the two is a key test of our models of structure formation. In particular, correlating the primordial map with the present locations of clusters and superclusters tests the evolution of structures, as potential wells only move due to nonlinear effects. Finally, cross-correlating the primordial map with tracers of the growth of structure is a new test that constrains the parameters of dark energy.

Acknowledgments: R.A. would like to thank N. Aghanim, J. C. A. Barata, M. Coutinho-Neto, T. Villela and C. A. Wuensche for valuable discussions. Financial support for this work has been provided by FAPESP and CNPq.

[1] C. L. Bennett *et al.*, Astrophys. J. Suppl. Ser. **148**, 1 (2003), astro-ph/0302207; D. Spergel *et al.*, Astrophys. J. Suppl. Ser. **148**, 175 (2003), astro-ph/0302209.

[2] D. Spergel *et al.*, arXiv: astro-ph/0603449.

[3] W. Percival *et al.*, *Mon. Not. Roy. Astron. Soc.* **327**: 1297 (2001), astro-ph/0105252; J. Peacock *et al.*, *Nature* **410**: 169 (2001), astro-ph/0103143; Licia Verde *et al.*, *Mon. Not. Roy. Astron. Soc.* **335**: 432 (2002), astro-ph/0112161.

[4] K. Abazajian *et al.*, *Astron. J.* **126**: 2081 (2003), astro-ph/0305492; M. Tegmark *et al. Phys. Rev.* **D69**: 103501 (2004), astro-ph/0310723; U. Seljak *et al.*, *Phys. Rev.* **D71**: 103515 (2005), astro-ph/0407372.

[5] V. Mukhanov, "Physical Foundations of Cosmology" (Cambridge University Press, 2005).

[6] S. Dodelson, "Modern Cosmology" (Academic Press, 2004).

[7] A. de Oliveira-Costa, M. Tegmark, M. Zaldarriaga and A. Hamilton, *Phys. Rev.* **D69**: 063516 (2004), astro-ph/0307282.

[8] G. Efstathiou, *Mon. Not. Roy. Astron. Soc.* **348**: 885 (2004), astro-ph/0310207.

[9] E. Gaztañaga *et al.*, *MNRAS* **346**: 47 (2003), astro-ph/0304178.

[10] C. J. Copi, D. Huterer, and G. D. Starkman, *Phys. Rev.* **D70**, 043515 (2004), astro-ph/0310511.

[11] D. Schwarz, G. Starkman, D. Huterer and C. Copi, *Phys. Rev. Lett.* **93**: 221301 (2004), astro-ph/0403353; C. Copi, D. Huterer, D. Schwarz and G. Starkman, *Mon. Not. Roy. Astron. Soc.* **367**:79 (2006), astro-ph/0508047.

[12] F. Hansen, P. Cabella, D. Marinucci and N. Vittorio, *Astrophys. J.* **607**: L67 (2004), astro-ph/0402396.

[13] H. Eriksen, F. Hansen, A. Banday, K. Górski and P. Lilje, *Astrophys. J.* **605**: 14 (2004), astro-ph/0307507.

[14] K. Land and J. Magueijo, *Phys. Rev. Lett.* **95**: 071301 (2005), astro-ph/0502237; *Mon. Not. Roy. Astron. Soc.* **362**: 838 (2005), astro-ph/0502574.

[15] A. Bernui, B. Mota, M. Rebouças and R. Tavakol, astro-ph/0511666.

[16] A. Bernui, T. Villela, C. Wuensche, R. Leonardi and I. Ferreira, astro-ph/0601593.

[17] A. de Oliveira-Costa and M. Tegmark, arXiv: astro-ph/0603369.

[18] C. Copi, D. Huterer, D. Schwarz, and G. Starkman, arXiv: astro-ph/0605135.

[19] L. R. Abramo *et al.*, *Phys. Rev.* **D74**: 063506 (2006), astro-ph/0604346.

[20] M. Kamionkowski and A. Loeb, *Phys. Rev.* **D56**: 4511 (1997), astro-ph/9703118.

[21] N. Seto and M. Sasaki, *Phys. Rev.* **D62**: 123004 (2000), astro-ph/0009222.

[22] A. Cooray and D. Baumann, *Phys. Rev.* **D67**: 063505 (2003), astro-ph/0211095; A. Cooray, D. Huterer and D. Baumann, *Phys. Rev.* **D69**: 027301 (2004), astro-ph/0304268; D. Baumann and A. Cooray, *New Astron. Rev.* **47**: 839 (2003), astro-ph/0304416.

[23] J. Portsmouth, *Phys. Rev.* **D70**: 063504 (2004), astro-ph/0402173.

[24] N. Seto and E. Pierpaoli, *Phys. Rev. Lett.* **95**: 101302 (2005), astro-ph/0502564.

[25] E. Bunn, *Phys. Rev.* **D73**: 123517 (2006) astro-ph/0603271.

[26] R. Sunyaev and Ya. B. Zel'dovich, *Astrophys. Space Sci.* **7**: 3 (1970); *Annu. Rev. Astron. Astrophys.* **18**: 537 (1980).

[27] Y. Rephaeli, *Annu. Rev. Astron. Astrophys.* **33**: 541 (1995); M. Birkinshaw, *Phys. Rep.* **310**: 97 (1999); J. Carlstrom, G. Holder and E. Reese, *Annu. Rev. Astron. Astrophys.* **40**: 643 (2002).

[28] S. Sazonov and R. Sunyaev, *MNRAS* **310**: 765 (1999).

[29] A. Yadav and B. Wandelt, *Phys. Rev.* **D71**: 123004 (2005), astro-ph/0505386.

[30] G. Holder, I. Iliev and G. Mellema, astro-ph/0609689.

[31] G.-C. Liu, A. da Silva and N. Aghanim, *Astrophys. J.* **621**: 15 (2005), astro-ph/0409295.

[32] A. Amblard and M. White, *New Astron.* **10**: 417 (2005), astro-ph/0409063.

[33] A. Cooray, D. Baumann and K. Sigurdson, astro-ph/0410006.

[34] M. Zaldarriaga and U. Seljak, *Phys. Rev.* **D58**: 023003 (1998), astro-ph/9803150.

[35] L. Page *et al.*, astro-ph/0603450.

[36] W. Reich, astro-ph/0603465.

[37] R. Leonardi *et al.*, *New Astron. Rev.* **50**: 977 (2006).

[38] A. Challinor, M. Ford and A. Lasenby, *MNRAS* **312**: 159 (2000), astro-ph/9905227.

[39] M. Shimon, Y. Rephaeli, B. O'Shea and M. Norman, *Mon. Not. Roy. Astron. Soc.* **368**: 511 (2006), astro-ph/0602528.

[40] P. Oxley *et al.*, *Proceedings of the SPIE* **5543**: 320 (2004), astro-ph/0501111.

[41] M. Myers *et al.*, *Appl. Phys. Lett.* **86**: 114103 (2005), http://bolo.berkeley.edu/polarbear/ .

[42] K. Yoon *et al.*, astro-ph/0606278; B. Keating *et al.*, *Proceedings of the SPIE* **4843** (2003); http://www.astro.caltech.edu∼lgg/bicep_front.htm.

[43] http://www.astro.caltech.edu∼lgg/spider_front.htm .

[44] M. Kesden, A. Cooray and M. Kamionkowski, *Phys. Rev. Lett.* **89**: 011304 (2002), astro-ph/0202434.

[45] C. Hirata and U. Seljak, *Phys. Rev.* **D68**: 083002 (2003); astro-ph/0306354; U. Seljak, C. Hirata, *Phys. Rev.* **D69** 043005 (2004), astro-ph/0310163.

[46] M. Zaldarriaga and U. Seljak, *Phys. Rev.* **D55**: 1830 (1997), astro-ph/9609170.

[47] M. Kamionkowski, A. Kosowsky and A. Stebbins, *Phys. Rev.* **D55**: 7368 (1997), astro-ph/9611125.

[48] W. Hu and M. White, *Phys. Rev.* **D56**: 596 (1997), astro-ph/9702170.

[49] G. Watson, "A Treatise on the Theory of Bessel Functions" (Cambridge U. Press, 1966).

[50] L. R. Abramo and H. Xavier, to appear.

[51] R. Penrose, *Proc. Cambridge Phil. Soc.* **51**: 406 (1955).